Electronic Supplementary Material (ESI) for Soft Matter.
This journal is © The Royal Society of Chemistry 2020

Supporting Information

Stratification of Polymer-Colloid Mixtures via Fast Nonequilibrium Evaporation

Kyoungmun Lee and Siyoung Q. Choi*

Department of Chemical and Biomolecular Engineering, Korea Advanced Institute of Science and Technology (KAIST), Daejeon 34141, Korea

SURFACE TENSION OF DRYING POLYMER SOLUTION

To confirm the evolution of polymer concentration gradient ($Pe_p > 1$) during the fast evaporation process, surface tension of the drying polymer solution (PVA M_w 18,000, $\phi_{i,p} = 0.04$) was measured. The evaporation was performed at ambient temperature and a relative humidity of 23%. As the evaporation progresses, surface tension of the drying solution $\gamma(t)$ (red circle) became much lower than the saturated surface tension ($\gamma_{saturated} \approx 60\ mN/m$) in Fig. S1(a). Thus, the polymers were accumulated near the drying interface in our experimental studies ($Pe_p > 1$).

In addition, the homogeneous polymer solution was compared with the drying solution in the pendant drop analysis. Ignoring non-reliable data points of the drying solution (within transparent red square, Bond number < 0.1[1]) in Fig. S1(a), $\gamma(t)$ starts to decrease much rapidly between 30 and 40 minutes. At 30 min after evaporation, the average volume fraction of the polymer ϕ_{avg} reaches 0.06, and it was compared with the homogeneous polymer solution ($\phi_{i,p} = 0.06$). As can be seen in Fig. S1(a), surface tension of the drying solution $\gamma(t = 30\ \text{min})$ (red circle) is lower than surface tension of the homogeneous solution ($\phi_{i,p} = 0.06$) (blue triangle). Thus, there are more polymers near the air/water interfaces (appearance of concentration gradient) in the drying solution than the homogeneous solution.

Moreover, the formation of concentration gradient in drying films was further supported by drainage of droplet in Fig. S1(b) and S1(c). Although both the drying and the homogeneous droplets have same average polymer volume fraction 0.06, they showed different behavior in drainage. For the drying solution [Fig. S1(b)], solid skin layer was observed in the drainage while nothing was remained in the homogeneous solution [Fig. S1(c)].

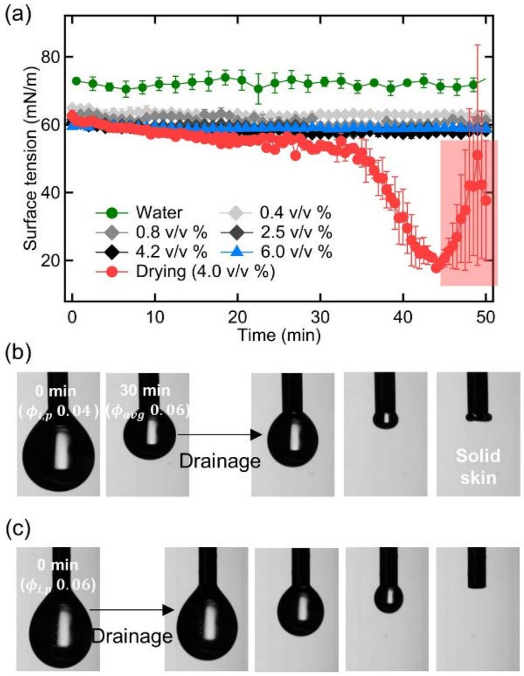

Fig. S1 (a) Surface tension of PVA M_w 18,000 solutions. Transition of surface tension of PVA M_w 18,000 ($\phi_{i,p} = 0.04$) was investigated to confirm the appearance of polymer concentration gradient near the drying interface. The surface tension of the drying solution became lower than saturated surface tension tension ($\gamma_{saturated} \approx 60\ mN/m$) as the evaporation progresses. Non-reliable data points are enclosed by red transparent square (Bond number < 0.1). (b) Droplet drainage after 30 min drying ($\phi_{i,p} = 0.04$, $\phi_{avg} = 0.06$). (c) Droplet drainage of homogeneous solution ($\phi_{i,p} = 0.06$).

RADUIS OF GYRATION OF POLYMER

Radius of gyration (R_g) of polymer in good solvent can be estimated by

$$R_g = \frac{1}{2} b n^{3/5}, \tag{S1}$$

where b is the length of each monomer, and n is the degree of polymerization. From the previous studies[2,3], R_g of poly(ethylene glycol) (PEG) and poly(vinyl alcohol) (PVA) can be calculated by Eq. (S1).

EVAPORATION RATE OF POLYMER-COLLOID MIXTURES

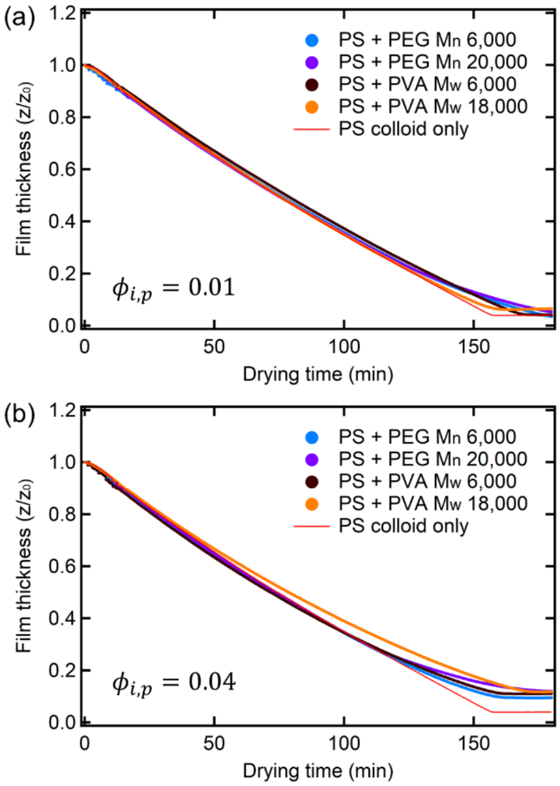

Fig. S2 Normalized film thickness of drying polymer-colloid mixtures. They show almost constant evaporation velocity v_{ev} except near the end of evaporation time. (a) $\phi_{i,p} = 0.01$ (b) $\phi_{i,p} = 0.04$. The evaporation rate v_{ev} was determined by the slope of the measured film thickness during 10 minutes of initial drying time.

DIFFUSION COEFFICIENT IN POLYMER/COLLOID MIXTURES

To determine diffusion coefficient of polymer in drying solutions, self-diffusion coefficient of polymer (D_s) was used rather than collective diffusion coefficient of polymer (D_c). Since all our experimental systems are in semi-dilute regime in good solvent at the initial state, collective motion of polymer would occur if there are no colloidal particles in solutions. However, there are lots of colloidal particles ($\phi_{i,p}: \phi_{i,c} = 3: 2$) simultaneously in our experimental systems. If colloidal particles can hinder the collective motion of polymers, polymers may not move collectively and might diffuse with disentanglement.

PEG and PVA can adsorb on the surface of PS colloids[4,5]. The adsorbed polymer act like glassy layer very near the colloidal surface and flexible layer far from the surface which move like bulk polymers[6,7]. This means that polymers can strongly adsorb on colloids and behave like polymer brushes grafted on colloidal surface. Thus, if there are colloids where polymers can adsorb in a system, bulk polymers can interact with colloidal-adsorbed polymers and slow-down the relaxation motion of bulk polymers near the colloids[7]. This interaction might hinder the collective motion of bulk polymers.

To further demonstrate the above argument, we compare the evolution time of polymer concentration gradient near the drying interface in homopolymer solution (PVA M_w 18,000 $\phi_p = 0.04$) and polymer-colloid mixtures (PVA M_w 18,000 $\phi_p = 0.04$ with $\phi_c = \phi_p \times \frac{2}{3}, \phi_p \times \frac{2}{30}, \phi_p \times \frac{2}{300}, \phi_p \times \frac{2}{3000}$) by measuring surface tension $\gamma(t)$ of the drying solutions (Fig. S3). Since the development of polymer concentration gradient is inversely proportional to the polymer diffusion constant, the slow-down of polymer diffusion due to the presence of colloids can be investigated by the evolution time of polymer concentration.

We can consider the reduction of $\gamma(t)$ is originated only from PVA because the $\gamma(t)$ of PS suspension is almost same with pure water (Fig. S3). Thus, the development of sufficiently high concentration gradient of PVA can be predicted by rapid reduction of $\gamma(t)$. In Fig. S3, the time when $\gamma(t)$ reaches minimum values decreases as the colloidal volume fraction increases. This indicates that colloids can accelerate the evolution of polymer gradient near the drying interfaces and disturb the diffusion of polymers.

In addition, slow diffusion of bulk polymer on polymer brush grafted surface was recently reported[8,9]. Zhang et al.[8] explored the diffusion of PEG within surface-grafted PEG layers in aqueous solution. Since they observed diffusion of PEG at very dilute regime, the measured diffusion coefficient of PEG can be considered as D_c. The good agreement of D_c of PEG near the PEG-grafted surface with D_s of the bulk PEG by considering brush concentration might imply that in our experimental studies, the diffusion of bulk polymer solutions may be slow down to D_s because of the polymers adsorbed on the colloids which hinder the collective motion of bulk polymers. Therefore, D_s of polymer is applied for the following modelling study.

Although many studies have been conducted on colloidal motion in polymer solutions[10,11], no studies on polymer diffusion in colloidal suspensions exists. Therefore, it is still unclear the reason for using D_s in polymer-colloid mixtures, but at least we confirmed that it can explain polymer-colloid stratification phenomena well. Indeed, in order to confirm the above hypothesis, diffusion of the polymer in colloidal suspensions is thought to require further study.

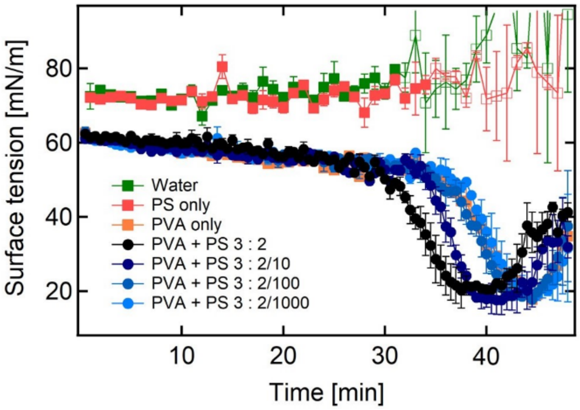

Fig. S3 Surface tension of PVA M_w 18,000 homopolymer solution ($\phi_p = 0.04$) and PVA M_w 18,000 + PS colloid mixtures ($\phi_p = 0.04$ and $\phi_c = \phi_p \times \frac{2}{3}, \phi_p \times \frac{2}{30}, \phi_p \times \frac{2}{300}, \phi_p \times \frac{2}{3000}$) under evaporation conditions. Ignoring non-reliable data (empty symbols, Bond number < 0.1), $\gamma(t)$ is almost same in PS suspensions and pure water. Thus, the concentration gradient of polymer near the drying interface can be observed by the reduction of $\gamma(t)$ in drying. As the volume fraction of PS colloids increases, a rapid reduction of $\gamma(t)$ occurs much faster.

DIFFUSION COEFFICIENT IN DRYING SOLUTIONS

The concentration dependence (or drying time dependence) of polymer diffusion coefficient D_p was determined using average volume fraction of polymer in drying films. Since the viscosity of polymer-colloid mixtures is similar with the viscosity of pure polymer solutions in Fig. S4, we only consider polymer concentration effect on the solution viscosity. In the non-draining limit, polymer chains behave as hard spheres and diffusion coefficient $D_p = k_B T / 6\pi\eta R_g$ can be estimated by the variation of viscosity[38]

$$\eta - \eta_s \sim \phi_p \qquad \text{(dilute, } 0 < \phi_p < \phi^*\text{)}, \tag{S2}$$

$$\eta - \eta_s \sim \phi_p^{1.3} \qquad \text{(semidilute unentangled, } \phi^* < \phi_p < \phi_e\text{)}, \tag{S3}$$

$$\eta - \eta_s \sim \phi_p^{3.9} \qquad \text{(semidilute entangled, } \phi_e < \phi_p < \phi^{**}\text{)}, \tag{S4}$$

$$\eta - \eta_s \sim \phi_p^{\alpha},\ \alpha > 3.9 \qquad \text{(concentrated, } \phi^{**} < \phi_p\text{)}, \tag{S5}$$

where ϕ^* is the solvent viscosity, ϕ^* is the overlap volume fraction, ϕ_e is the entanglement volume fraction, and ϕ^{**} is the volume fraction of polymer when it reaches concentrated regime. Since initial conditions that we used ($\phi_{i,p} = 0.01, 0.04$) is in semidilute regime (Fig. 4), we do not consider the range in dilute regions.

During the evaporation with constant v_{ev}, average volume fraction of polymer can be written as

$$\phi_{p,avg} = \frac{V_i \phi_{i,p}}{V_i - \frac{v_{ev}}{z_0} V_i t}, \tag{S6}$$

$$\frac{\phi_{p,avg}}{\phi_{i,p}} = \frac{1}{1-t^*}, \tag{S7}$$

where V_i is initial volume of polymer solution and $t^* = t v_{ev}/z_0$ $(0 \le t^* \le 1)$ is the dimensionless time. Before the polymer solution enters semidilute entangled regime ($\phi_{i,p} < \phi_e$), the viscosity is

$$\frac{\eta - \eta_s}{\eta_i - \eta_s} = \left(\frac{\phi_{p,avg}}{\phi_{i,p}}\right)^{1.3}, \tag{S8}$$

$$\eta = \left(\frac{\phi_{p,avg}}{\phi_{i,p}}\right)^{1.3} (\eta_i - \eta_s) + \eta_s, \tag{S9}$$

$$\eta = \left(\frac{1}{1-t^*}\right)^{1.3} (\eta_i - \eta_s) + \eta_s. \tag{S10}$$

If the average polymer volume fraction reaches ϕ_e,

$$\frac{\phi_{p,avg}}{\phi_e} = \frac{\phi_{p,avg}/\phi_{i,p}}{\phi_e/\phi_{i,p}} = \frac{1/(1-t^*)}{1/(1-t_e^*)} = \frac{1-t_e^*}{1-t^*}, \tag{S11}$$

where t_e^* is the dimensionless time when $\eta = \eta_e$ (viscosity when $\phi_p = \phi_e$) during drying from Eq. (S10). Within the semidilute entangled regime (($\phi_e < \phi_{p,avg} < \phi^{**}$), η can be determined by

$$\frac{\eta - \eta_s}{\eta_e - \eta_s} = \left(\frac{\phi_{p,avg}}{\phi_e}\right)^{3.9}, \tag{S12}$$

$$\eta = \left(\frac{\phi_{p,avg}}{\phi_e}\right)^{3.9} (\eta_e - \eta_s) + \eta_s, \tag{S13}$$

$$\eta = \left(\frac{1-t_e^*}{1-t^*}\right)^{3.9} (\eta_e - \eta_s) + \eta_s. \tag{S14}$$

Similarly, Pe_p is determined by the substitution of D_p in $Pe_p = v_{ev} z_0 / D_p$.

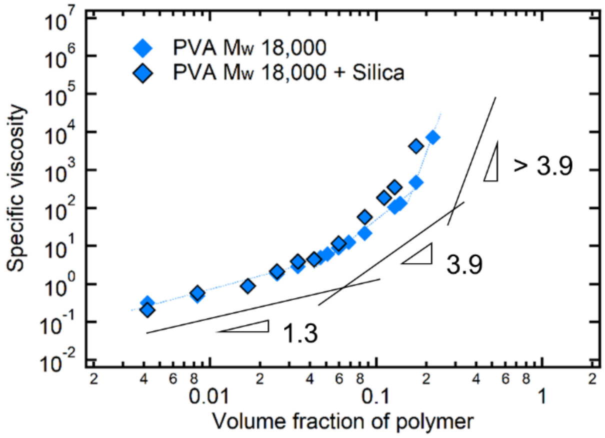

Fig. S4 Specific viscosity of polymer-colloid mixture and pure polymer solution. The viscosity of PVA M_w 18,000 + Silica is almost similar with PVA M_w 18,000 before it goes to concentration regime, where the slope changes from 3.9 to larger than 3.9.

CRITERIA FOR REGIME 3 ($t_s^* \approx 1$)

To determine whether the system is in regime 3 (how close should t_s^* be to 1), the length of initial accumulation zone $D_{i,p}/v_{ev}$, where $D_{i,p}$ is the initial diffusion coefficient of polymer, was compared with remained film height $(1 - t^*)z_0$ at $t^* = t_s^*$. If the initial accumulation zone already reaches bottom substrate at $t^* = t_s^*$, we consider that the system belongs to regime 3. For regime 3,

$$(1 - t_s^*)z_0 < D_{i,p}/v_{ev}, \tag{S15}$$

$$t_s^* > 1 - 1/Pe_{i,p}. \tag{S16}$$

Among the 8 systems, 4 systems having $\phi_{i,p} = 0.01$ are close to regime 3 (Fig. S5).

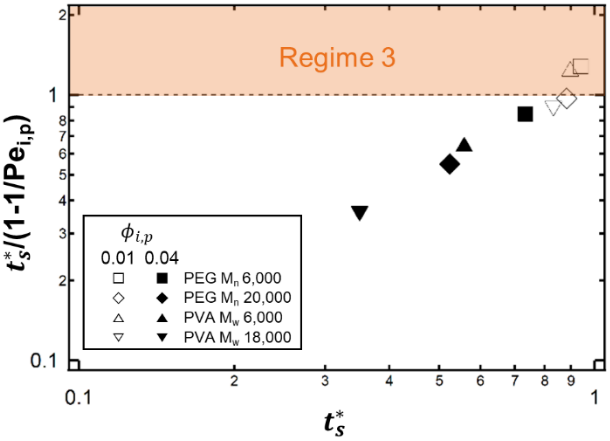

Fig. S5 Comparison of the initial accumulation zone and remained film height at $t^* = t_s^*$. Systems having $\phi_{i,p} = 0.01$ show very close to regime 3, while t_s^* of $\phi_{i,p} = 0.04$ systems quite far from $1 - 1/Pe_{i,p}$.

AIR/WATER INTERFACIAL ACTIVITY OF PVA M_w 6,000

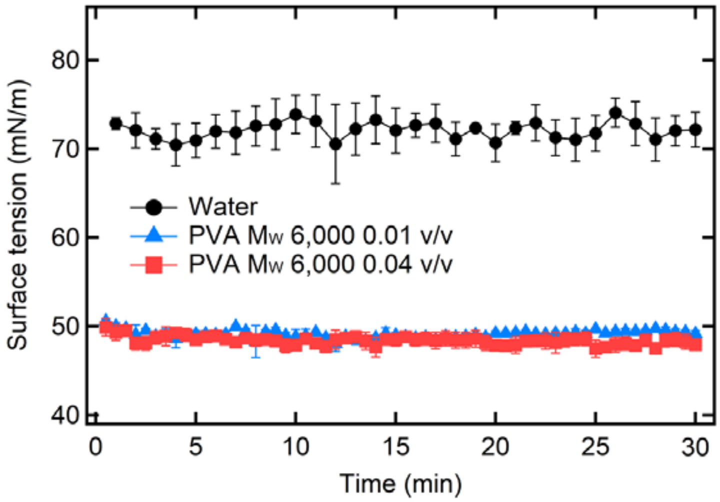

Fig. S6 Surface tension of PVA M_w 6,000 solution. Both ϕ_p = 0.01 and 0.04 shows similar surface tension value. This means that interfacial activity of PVA M_w 6,000 was almost saturated before the ϕ_p reached 0.01. In addition, PVA M_w 6,000 goes to air/water interface within a very short time (< 3 min).

TRANSITION TO ANOTHER EXPERIMENTAL PARAMETER OF t_c^* AND t_s^*

Expressions of t_c^* and t_s^* are represented as another experimental parameters. For simplicity of mathematical calculations, we set the dimensionless time t_c^* as

$$\phi_p\left(z_{interface}, t_c^*\right) = \phi_p^{**}, \tag{S17}$$

$$\phi_p(z_{interface}, t_c^*) \approx \phi_{i,p}(1 + Pe_p(t_c^*)t_c^*) = \phi_p^{**}, \tag{S18}$$

$$t_c^* \approx \frac{\frac{\phi^{**}}{\phi_{i,p}} - 1}{Pe_p(t_c^*)}, \tag{S19}$$

where $Pe_p(t_c^*)$ is Pe of polymer at dimensionless time $t^* = t_c^*$.

In similar way, t_s^* can be written as

$$v_{colloid,interface}(t_s^*) = v_{ev}, \tag{S20}$$

$$v_{colloid,interface}(t_s^*) \approx \frac{9}{4} v_{ev}\phi_{i,p}\left(1 + Pe_p(t_s^*)t_s^*\right) = v_{ev}, \tag{S21}$$

$$t_s^* \approx \frac{\frac{4}{9}\frac{1}{\phi_{i,p}} - 1}{Pe_p(t_s^*)}, \tag{S22}$$

where $Pe_p(t_s^*)$ is Pe of polymer at dimensionless time $t^* = t_s^*$.

GRAVITY EFFECT ON STRATIFICATION

For the formation of stratified layers in dried films which cannot achieve stratification only by changing v_{ev}, gravitation effect was investigated. Theoretical calculation of t_S^* was performed with the assumption that medium density ρ_0 is almost constant during drying ($\rho_0 \approx 1\ g/ml$). The transition of medium viscosity η was only considered for the additional gravitational velocity v_g. Gravitational velocity v_g is

$$v_g = -\frac{2r^2(\rho-\rho_0)g}{9\eta}, \tag{S23}$$

where r is radius of colloid, ρ is colloidal density and g is gravitational acceleration. Thus, the velocity of interfacial colloids with the addition of gravitational effect can be written as

$$v_{grav-colloid,interface} \approx \frac{9}{4} v_{ev}\phi_{i,p}\left(1 + Pe_p t^*\right) + \ v_g. \tag{S24}$$

We determine that t_s^* emerges when $v_{grav-colloid,interface} = v_{ev}$ and t_c^* equals the value without considering gravitational velocity.

In case of PS colloid that was used in Fig. 1 and Fig. 2, v_g can be neglected since the density of PS ($\rho_{PS} = 1.05\ g/ml$) is quite similar to the water density ($\rho_{water} = 1.00\ g/ml$). If the type of colloid is changed to silica ($\rho_{silica} = 2$ g/ml) with PVA M_w 18,000 ($\phi_{i,p} = 0.04$), t_c^*/t_s^* goes next to 1 and this can change final dried film morphology from nonstratified layer to clearly stratified layer in Fig. S7.

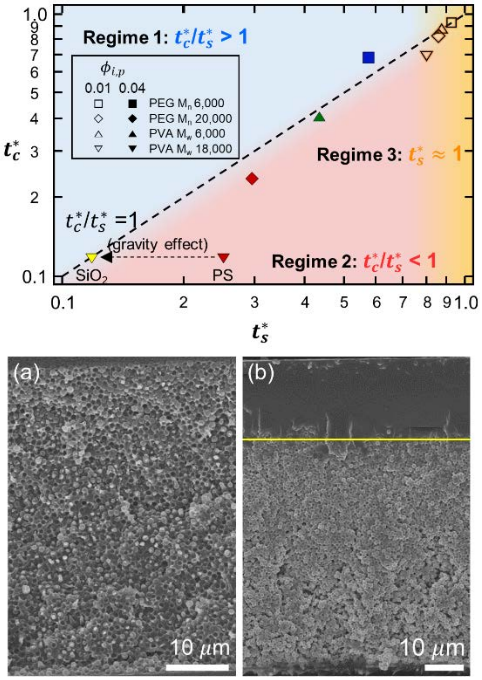

Fig. S7 Gravity effect on stratification of polymer-colloid mixtures (PVA M_w 18,000, $\phi_{i,p} = 0.04$, $\phi_p : \phi_c = 3:2$). All the experimental conditions are same except for the colloidal type, (a) PS ($\rho_{PS} = 1.05$ g/ml) and (b) Silica ($\rho_{silica} = 2.00$ g/ml). For the theoretical calculation, the gravitational velocity from density difference is added to $v_{colloid,interface}$. SEM image of (a) is same with Fig. 2(d). Clear stratification can be observed in colloidal silica and polymer mixture, while randomly distributed structure was obtained in colloidal PS and polymer mixture.

DETAILS OF THE EXPERIMENTS

A. Materials

Glass slide substrates of 27 mm × 76 mm in size were purchased from Duran. Ultrapure water was produced by Millipore ICW-3000 water purification system (> 18 MΩ). Polystyrene microsphere with a diameter of 1.0 μm (± 0.04 μm-s.d., 10.14% solid content in water) was provided by Bang's laboratories, Inc. and 1.0 μm silica particles (± 0.05 μm-s.d., 10% solid content in water) was purchased from Polysciences, Inc. Both PS and silica colloidal particles purified at least three times with deionized water. It was first centrifuged, and then supernatant was replaced by purified water. Zeta potential on PS colloid and silica colloid are -23.8 mV (± 0.2 mV) and -74.4 mV (± 3.5 mV) relatively. Poly(ethylene glycol) (PEG) M_n (number average molecular weight) 6,000 gmol^{-1}, PEG M_n 20,000 gmol^{-1}, and poly(vinyl alcohol) (PVA) M_w (weight average molecular weight) 13,000-23,000 gmol^{-1} (degree of hydrolysis 98%) were purchased from Sigma-Aldrich. PVA M_w 6,000 gmol^{-1} (degree of hydrolysis 80%) was purchased from Polysciences, Inc. All the polymers used have larger molecular weight than entanglement molecular weight (PEG is as high as 2,200 g/mol PVA is as high as 5,800 g/mol). Although PVA M_w 6,000 is very near the entanglement limit, it shows entangled dynamics similar with other polymer solutions (Fig. 3). The desired concentration of PVA solution was prepared by heating the PVA-water mixtures at 85^oC for 1 h, then cooling the system to ambient temperature. Highly concentrated PVA solution was heated at 85^oC for 12 h to obtain homogeneous solutions.

B. Dried film formation

Glass substrates (10 mm × 10 mm) were cleaned in acetone in a sonicating bath for 10 min. They were dried using nitrogen gas and placed in a drying oven (Changshin Science) for 3 min to completely remove acetone. To achieve the required volume ratio ($\phi_p : \phi_c = 3 : 2$), polymers and colloids were mixed to prepare polymer-colloid mixtures, which was then diluted by the addition of deionized water until the desired initial concentration. Volume fraction of polymer in solution calculated by density at solid state. Solution mixtures of polymer-colloid were deposited on the glass substrates with an initial wet thickness of approximately 1.25 mm. The samples were dried at ambient temperature with a relative humidity of 23% (measured by TFA digital thermos-hygrometer, Daedeok scientific), leading to the Pe > 1 for both the colloid and polymer. Relative humidity was achieved by placing a bottle filled with water or purging with N_2 gas in the drying chamber.

C. Structure characterization

The final morphology of dried films was characterized by observing the cross-sectional images through the scanning electronic microscopy (SEM) (Hitachi, Japan). Cross-sectional films were prepared by cutting a completely dried film after scratching the glass with diamond glass cutter (4science, South Korea). The samples were coated with Osmium coater (HPC-1SW, Vacuum Device) before taking images to prevent charging effect. In addition, imaging processing of SEM images in ImageJ software further analyzed the spatial distribution of polymers and colloids. SEM images firstly separated to 30 parts in vertical to calculate volume fraction of polymer (ϕ_p) and colloid (ϕ_c) by film height. All the ϕ_c in SEM images are collected by sphere shape or brightness difference through the ImageJ analysis. All samples in Fig. 1 characterize ϕ_c by brightness difference and ϕ_c in Fig. 2 characterized by sphere shape. The remained volume fraction was considered as polymer volume fraction ($\phi_p = 1 - \phi_c$). The threshold lines, which denoted as yellow line in Fig. 1 and Fig. 2, to distinguish between the phases were regarded as the minimum height when $\phi_p \geq \phi_c$.

D. Dynamic viscosity of polymer solutions

After preparing polymer solutions of various concentrations (two molecular weights of both PEG and PVA, from 0.5 to 30 - 60 v/v% depending on the system), rheological properties were identified using a conventional rheometer (MCR 302, Anton Paar, Austria) with cone plate geometry (0.1 mm gap, 50 mm diameter). The viscoelastic properties of each solution were characterized by dynamic viscosity measurements within the shear rate range from 0.01 s^{-1} to 1000 s^{-1}. Most dispersions exhibited Newtonian fluid behavior within the measured shear rate and the viscosity value at the lowest shear rate was considered zero shear viscosity.

Notes and references

1 Joseph D. Berry, Michael J. Neeson, Raymond R. Dagastine, Derek Y. C. Chan and Rico F. Tabor, *J. Colloid Interf. Sci.*, 2015, **454**, 226.
2 Charmainne Cruje and Devika B. Chithrani, *J. Nanomed. Res.*, 2014, **1**, 01.
3 Mitsuhiro Shibayama, Hidenobu Kurokawa, Shunji Nomura, M. Muthukumar, Richard S. Stein and Saroj Roy, *Polymer*, 1992, **33**, 2883.
4 M. S. AHMED, M. S. EL-AASER and J. W. VANDERHOFF, *ACS Symp. Ser.*, 1984, **240**, 77.
5 Janet A. Kling and Haryy J. Ploehn, *J. Colloid. Interf. Sci.*, 1998, **198**, 241.
6 So Youn Kim, Kenneth S. Schweizer and Charles F. Zukoski, *Phys. Rev. Lett.*, 2011, **107**, 225504.
7 So Youn Kim, Henriette W. Meyer, Kay Saalwachter and Charles F. Zukoski, *Macromolecules*, 2012, **45**, 4225.
8 Zhenyu J. Zhang, Steve Edmondson, Matthew Mears, Jeppe Madsen, Steven P. Armes, Graham J. Leggett and Mark Geoghegan, *Macromolecules*, 2018, **51**, 6312.
9 Christopher G. Clarkson, Alexander Johnson, Graham J. Leggett and Mark Geoghegan, *Nanoscale*, 2019, **11**, 6052.
10 C. -Y. Chou, B. C. Eng and M. Robert, *J. Chem. Phys.*, 2006, **124**, 044902.
11 Yunhong Dong, Xiaoqing Feng, Nanrogn Zhao and Zhonghuai Hou, *J. Chem. Phys.*, 2015, **143**, 204903.